

M. Sekido · T. Fukushima

A VLBI delay model for radio sources at a finite distance

Received: 22 June 2005 / Accepted: 22 February 2006 / Published online: 28 April 2006
© Springer-Verlag 2006

Abstract A relativistic delay model for Earth-based very long baseline interferometry (VLBI) observation of sources at finite distances is derived. The model directly provides the VLBI delay in the scale of terrestrial time. The effect of the curved wave front is represented by using a pseudo source vector $\mathbf{K} = (\mathbf{R}_1 + \mathbf{R}_2)/(R_1 + R_2)$, and the variation of the baseline vector due to the difference of arrival time is taken into account up to the second-order by using Halley's method. The precision of the new VLBI delay model is 1 ps for all radio sources above 100 km altitude from the Earth's surface in Earth-based VLBI observation. Simple correction terms (parallax effect) are obtained, which can also adopt the consensus model (e.g. International Earth Rotation and Reference Frames Service conventions) to finite-distance radio source at $R > 10$ pc with the same precision. The new model may enable estimation of distance to the radio source directly with VLBI delay data.

Keywords Very Long Baseline Interferometry · General Theory of Relativity · Spacecraft Navigation

1 Introduction

Very long baseline interferometry (VLBI) is a powerful tool for astronomy and space geodesy, boasting the highest angular resolution. In fact, the International Celestial Reference Frame is realized by VLBI observation of extragalactic objects and its overall precision was reported as $250 \mu\text{s}$ for the

position of individual sources and $20 \mu\text{as}$ for the axis orientation of the reference frame (Charlot 2004). Furthermore, a phase-reference-dedicated VLBI project, VLBI Exploration of Radio Astrometry (VERA; Kobayashi 2004), has started and its target precision is set at the $10 \mu\text{as}$ level.

On the other hand, the VLBI technique has been used for spacecraft navigation as its engineering application (Border et al. 1982). Recently, the technique was used for the angular observation of some closer targets such as NOZOMI, a Japanese Mars exploration mission (Yamamoto and Tsuruda 1998), and Cassini-Huygens, which is a joint European Space Agency (ESA)–National Aeronautics and Space Administration (NASA) probe to Saturn's satellite Titan (Lebreton and Matson 2002). Soon VLBI will be applied to SELENE, a Japanese Lunar gravimetry mission (Matsumoto, et al. 1999; Heki et al. 1999).

To utilize the full power of VLBI, the establishment of precision VLBI delay model is essential. For sources at practically infinite distances, such as quasars, various models have been proposed (Hellings 1986; Shahid-Saless and Hellings 1991; Zhu and Groten 1988; Soffel et al. 1991). They were unified into the so-called *consensus model* (Eubanks 1991). It has a 1 ps precision for Earth-based VLBI observation of extra-galactic radio sources. Resolution B1.3 of the International Astronomical Union (IAU) XXIV General Assembly (2000) recommends use of the Barycentric Celestial Reference System (BCRS) and Geocentric Celestial Reference System (GCRS) for the barycentric and geocentric reference systems in the framework of general relativity. The consensus model has reviewed and adapted to the substantial framework of the IAU-recommended BCRS, and has been used in the International Earth Rotation and Reference Systems Service (IERS) conventions (McCarthy and Petit 2003) and in the world VLBI community as the standard VLBI delay model.

Unfortunately, this model was designed for extra-galactic radio sources and was derived based on the plane-wave approximation by ignoring the effect of source's distance (Eubanks 1991). Therefore, it is inaccurate if the radio sources are at finite distance, e.g. pulsars (maser sources in our

M. Sekido (✉)
Kashima Space Research Center,
National Institute of Information and Communications Technology,
893-1 Hirai, Kashima, Ibaraki 314-0012, Japan
E-mail: sekido@nict.go.jp,
Tel.: +81-299-84-7146
Fax: +81-299-84-7159

T. Fukushima
National Astronomical Observatory,
2-21-1 Osawa Mitaka, Tokyo 181-8588, Japan
E-mail: Toshio.Fukushima@nao.ac.jp

galaxy), and the error is intolerable for radio sources in the Solar System. When the distance to the radio sources is less than about 200 kpc (kilo-parsec), the inaccuracy exceeds 1 ps for a 12,000 km VLBI baseline due to the effect of the curved wave-front.

Moyer (2000) provides a VLBI delay model for spacecraft observation. It is based on numerical solution of the light-time equation for two ray paths from one radio source to two observers. However it may not be suitable for pulsars and other objects outside the Solar System, since most parts of two ray paths from radio source to observers are common in that case. Alternative schemes to obtain the VLBI delay for finite-distance radio sources were investigated by Klioner (1991), Sovers et al. (1998), and Fukushima (1994). Fukushima (1994) presented a vector formula, by which the VLBI delay for a finite-distance radio source can be expressed in the same form as an infinite one. The VLBI delay is given by numerical iteration in his model. Klioner (1991) proposed an analytical formula for the VLBI delay model for radio sources in the Solar System. His formula is equivalent with ours in the BCRS at the order of $(V_E/c)^2$ (Sect. 3.1).

However both representations of the VLBI delay by Fukushima and Klioner are given in BCRS. As such, time intervals in that coordinate system have to be transformed to proper time at the observer's location for data processing. This is because current VLBI data analysis software [e.g. CALC/SOLVE (Petrov 2005), OCCAM (Titov 2004)] traditionally deal with data in the time scale of terrestrial time (TT), instead of converting observed data from proper time at the observer's location to barycentric coordinate time (TCB). In addition, the consensus model is used to provide VLBI delays in the TT-scale.

Motivated by the potential need of VLBI analysis of spacecraft coordinates (Sekido et al. 2004), we have derived an analytical representation of VLBI delay expressed in the TT-scale with an accuracy of 1 ps for ground-based VLBI observation of radio sources at finite distances. This model is considered to be an expansion of the consensus model, and it is useful for implementation in current VLBI analysis software.

We first introduce the barycentric dynamical time (TDB) and TT frames for derivation of the formula. These reference systems are identical with BCRS and GCRS, except for a scale difference. Motions of spacecraft and other radio sources at finite distance may be described in a dynamical celestial reference frame. In practice, such a reference frame is the planetary ephemeris (such as the JPL ephemeris). Therefore, derivation of the formula with the TDB-frame, which the JPL ephemeris is based on, is better for a practical understanding.

In Sect. 2, the celestial reference system used as the base of formulation is introduced and the new VLBI delay model is presented. A full derivation scheme is described in Appendix A. Comparison with other VLBI delay models is discussed in Sect. 3.

2 Finite distance VLBI delay model

2.1 Coordinate system of reference

A reference system should be chosen so that the physical process of concern can be described as simply as possible. Resolution B1.3 adopted at the XXIV IAU General Assembly (hereafter IAU-GA-XXIV) recommends the choice of harmonic coordinates of the barycentric and the geocentric reference system (Soffel et al. 2003). The former one is called the BCRS, whose time-coordinate is called TCB. It is suitable for describing events in the Solar System. The latter one is called GCRS, whose time-coordinate is called geocentric coordinate time (TCG). This is used for describing local events nearby earth.

The metric tensor of BCRS is explicitly given by

$$\begin{aligned} g_{00} &= -1 + \frac{2W(T, \mathbf{X})}{c^2} - \frac{2W(T, \mathbf{X})^2}{c^4} \\ g_{0i} &= -\frac{4}{c^3} W^i(T, \mathbf{X}) \\ g_{ij} &= \delta_{ij} \left(1 + \frac{2}{c^2} W(T, \mathbf{X}) \right) \end{aligned} \quad (1)$$

with

$$\begin{aligned} W(T, \mathbf{X}) &= G \sum_J \int \frac{\sigma(T, \mathbf{X}')}{|\mathbf{X} - \mathbf{X}'|} d^3 X' \\ &\quad + \frac{1}{2c^2} G \sum_J \frac{\partial^2}{\partial T^2} \int \sigma(T, \mathbf{X}') |\mathbf{X} - \mathbf{X}'| d^3 X' \\ W^i(T, \mathbf{X}) &= G \sum_J \int \frac{\sigma^i(T, \mathbf{X}')}{|\mathbf{X} - \mathbf{X}'|} d^3 X', \end{aligned} \quad (2)$$

where $W(T, \mathbf{X})$ is scalar potential and $W^i(T, \mathbf{X})$ is vector potential. As a boundary condition, both of the potentials vanish far from the Solar System. Space-time coordinates of BCRS are presented by (T, \mathbf{X}) . Suffix $i, j = 1, 2, 3$ and J runs over all gravitating bodies in the Solar System. σ and σ^i are gravitational mass and current density. G and c are gravitational constant and speed of light, respectively. δ_{ij} is Kronecker's delta.

The metric tensor of GCRS is also explicitly given in IAU-GA-XXIV resolution B1.3 as

$$\begin{aligned} G_{00} &= -1 + \frac{2w(t, \mathbf{x})}{c^2} - \frac{2w(t, \mathbf{x})^2}{c^4} \\ G_{0i} &= -\frac{4}{c^3} w^i(t, \mathbf{x}) \\ G_{ij} &= \delta_{ij} \left(1 + \frac{2}{c^2} w(t, \mathbf{x}) \right) \end{aligned} \quad (3)$$

with

$$\begin{aligned} w(t, \mathbf{x}) &= w_E(t, \mathbf{x}) + w_{\text{ext}}(t, \mathbf{x}) \\ w^i(t, \mathbf{x}) &= w_E^i(t, \mathbf{x}) + w_{\text{ext}}^i(t, \mathbf{x}), \end{aligned} \quad (4)$$

where geocentric potential is split into gravitational potential due to the Earth $w_E(t, \mathbf{x})$, $w_E^i(t, \mathbf{x})$, and external parts

$w_{\text{ext}}(t, \mathbf{x})$, $w_{\text{ext}}^i(t, \mathbf{x})$, which are due to tidal and inertial effects. Geocentric space-time coordinates of the GCRS is represented by (t, \mathbf{x}) . $w_E(t, \mathbf{x})$ and $w_E^i(t, \mathbf{x})$ are defined in the same way with $W(T, \mathbf{X})$ and $W^i(T, \mathbf{X})$, but calculated in the GCRS with integrals taken over the whole Earth. As boundary condition, the external parts of the potential are assumed to vanish at the geocenter.

The observed time interval of a VLBI delay is measured in the time-scale of proper-time at the observer. Proper-time at each observation station differs from TT due to differences in location on the Earth. Although such differences of local time scales are practically absorbed by the time synchronization procedure used to adjust the clock rate to that of Temps Atomique Internationale (TAI), which is thought of as a realization of TT. Thus we can suppose that the observed delay is measured in the TT-scale. TT is re-defined by IAU-GA-XXIV resolution B1.9 such that it is a time-scale differing from TCG by a constant rate:

$$\frac{d \text{TT}}{d \text{TCG}} = 1 - L_G, \quad (5)$$

where $L_G = 6.969290134 \times 10^{-10}$ is a defining constant (McCarthy and Petit 2003, p. 126) corresponding to W_G/c^2 where W_G is the potential on the geoid.

For practical reasons, here we define the TT-frame as a geocentric celestial reference system differing from GCRS by a constant scaling factor of $1 - L_G$. The metric of the TT-frame is expressed by using the metric tensor of Eq. (3) as

$$ds^2 = (1 - L_G)^{-2} (G_{00} c^2 d\tau^2 + G_{ij} d\xi^i d\xi^j + 2G_{0k} d\xi^k c d\tau), \quad (6)$$

where i, j, k runs for 1, 2, and 3. Space-time coordinates of the TT-frame are denoted by (τ, ξ) . Throughout this paper, the following rule will be applied. Repeated indexes in an equation means taking summation for that index (Einstein's summation). The scalar product of vectors \mathbf{a} and \mathbf{b} may be represented by $\mathbf{a} \cdot \mathbf{b} = a^i b^i$.

Spatial scale on the International Terrestrial Reference System (ITRS), which is the coordinate system fixed on the crust of the Earth, is defined to be consistent with TCG (TCG-scale) (McCarthy and Petit 2003, p. 25). However, its realization, the International Terrestrial Reference Frame (ITRF), is not always consistent with the TCG-scale. The most recent version, ITRF2000, is given by a spatial scale consistent with time scale of TT (TT-scale), but earlier versions ITRF94, ITRF96, and ITRF97 are expressed in the TCG-scale (McCarthy and Petit 2003, Sects. 4.2.2 and 4.2.4). In this paper, we assume that the station's coordinates are given in the TT-frame. Coordinate transformation from ITRF to the TT-frame is performed by

$$[\text{TT-frame}] = Q(t)R(t)W(t)[\text{ITRF}], \quad (7)$$

where the rotation matrices $Q(t)$, $R(t)$, and $W(t)$ are given by McCarthy and Petit (2003, Sect. 5).

Coordinates of a space object in the Solar System are given in planetary ephemerides such as DE405 (Standish,

1998a) which is thought of as a realization of the barycentric dynamical reference system. In fact, the Jet Propulsion Laboratory (JPL) planetary (DE405) and lunar (LE405) ephemerides are regarded as dynamical realizations of the ICRS (McCarthy and Petit 2003, Sect. 3). The time argument T_{eph} of the JPL ephemerides is not TCB, but a coordinate time that is related to TCB by an offset and a constant rate. Since these ephemerides are automatically adjusted in the creation process so that the rate of T_{eph} has no overall difference from the rate of TT (Standish 1998b), then T_{eph} is consistent with the definition (Guinot and Seidelmann 1988) of TDB. Therefore T_{eph} can be thought as a realization of TDB.

The constant scaling factor is represented by

$$1 - L_B \stackrel{\text{def}}{=} \left\langle \frac{d \text{TT}}{d \text{TCB}} \right\rangle = \frac{dT_{\text{eph}}}{d \text{TCB}} = \frac{d \text{TT}}{d \text{TCG}} \left\langle \frac{d \text{TCG}}{d \text{TCB}} \right\rangle = (1 - L_G)(1 - L_C), \quad (8)$$

where $\langle \rangle$ represents an average for a sufficiently long time period.

$$1 - L_C \stackrel{\text{def}}{=} \left\langle \frac{d \text{TCG}}{d \text{TCB}} \right\rangle \quad (9)$$

A recent estimate of L_C is (Irwin and Fukushima 1999)

$$L_C = 1.48082686741 \times 10^{-8} \pm 2 \times 10^{-17}. \quad (10)$$

From Eqs. (8) and (10) and the value of the defining constant L_G , here we use a constant factor $L_B = 1.55051976772 \times 10^{-8}$.

Hereafter we call the reference frame of the JPL planetary ephemeris the TDB-frame, which is a barycentric reference frame differing from BCRS by a constant scaling factor L_B . The metric of the TDB-frame is expressed with metric tensor (cf. Eq. 1) as

$$ds^2 = (1 - L_B)^{-2} (g_{00} c^2 d\tilde{T}^2 + g_{ij} d\tilde{X}^i d\tilde{X}^j + 2g_{0k} d\tilde{X}^k c d\tilde{T}), \quad (11)$$

where $(\tilde{T}, \tilde{\mathbf{X}})$ is space-time coordinates of TDB-frame.

2.2 VLBI delay model for radio source at finite distance

The problem to be solved is representation of time interval $\tau_2 - \tau_1$ in TT with baseline vector and radio source coordinates, under the condition that the motions of Earth and radio source are given as functions of time. Let us consider that a radio signal departing from a source S at $(\tilde{T}_0, \tilde{\mathbf{X}}_0)$ arrives at stations 1 and 2, respectively, at $(\tilde{T}_1, \tilde{\mathbf{X}}_1)$ and $(\tilde{T}_2, \tilde{\mathbf{X}}_2)$ in the TDB-frame (Fig. 1). The same events of signal arrival to station i is indicated by (τ_i, ξ_i) in the TT-frame.

Here we define a pseudo source vector \mathbf{K} (Fukushima 1994) as

$$\mathbf{K} \stackrel{\text{def}}{=} \frac{\mathbf{R}_1(\tilde{T}_1) + \mathbf{R}_2(\tilde{T}_1)}{R_1(\tilde{T}_1) + R_2(\tilde{T}_1)} \quad (12)$$

with

$$\begin{aligned} \mathbf{R}_i(\tilde{T}_1) &= \tilde{\mathbf{X}}_0(\tilde{T}_0) - \tilde{\mathbf{X}}_i(\tilde{T}_1) \\ &= \tilde{\mathbf{X}}_0(\tilde{T}_0) - \tilde{\mathbf{X}}_E(\tilde{T}_1) - \mathbf{R}_{iE}(\tilde{T}_1), \end{aligned} \quad (13)$$

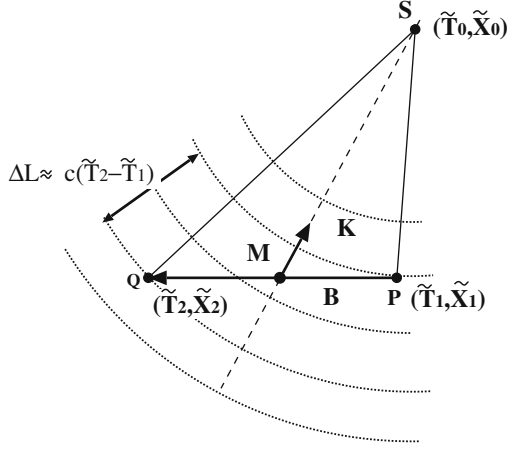


Fig. 1 Configuration of VLBI observation for a radio source at finite distance. The signal emitted from the radio source S at $(\tilde{T}_0, \tilde{\mathbf{X}}_0)$ arrives at the observation station 1 (designated as P) and 2 (Q) at $(\tilde{T}_1, \tilde{\mathbf{X}}_1)$ and $(\tilde{T}_2, \tilde{\mathbf{X}}_2)$, respectively. The pseudo direction vector \mathbf{K} defined by Eq. (76) is on the line from the middle point of the baseline \mathbf{B} to the source S in the TDB-frame

$$R_i(\tilde{T}_1) = |\mathbf{R}_i(\tilde{T}_1)| \quad (14)$$

where $\mathbf{R}_{iE}(\tilde{T}_1)$ is vector from the geocenter $(\tilde{T}_1, \tilde{\mathbf{X}}_E)$ to station i ($= 1, 2$) in the TDB-frame, and it is expressed with station coordinates in the TT-frame (τ_i, ξ_i) as

$$\mathbf{R}_{iE}(\tilde{T}_1) = \left(1 - \frac{W_E}{c^2} - L_C\right) \xi_i(\tau_1) - \left(\frac{\mathbf{V}_E \cdot \xi_i(\tau_1)}{2c^2}\right) \mathbf{V}_E, \quad (15)$$

where W_E is the gravitational scalar potential of Eq. (2) evaluated at the geocenter $(\tilde{T}_1, \tilde{\mathbf{X}}_E)$, but the summation is taken for all gravitating bodies except for the Earth. \mathbf{V}_E is the coordinate velocity vector of the Earth at \tilde{T}_1 . We suppose the coordinates of a spacecraft in the TDB-frame $\tilde{\mathbf{X}}(\tilde{T})$ is given as the function of \tilde{T} .

$$\begin{aligned} & (\tau_2 - \tau_1)_{\text{finite}} \\ &= \frac{\left\{ - \left[1 - 2 \frac{W_E}{c^2} - \frac{|\mathbf{V}_E|^2 + 2\mathbf{V}_E \cdot \mathbf{v}_2}{2c^2} \right] \frac{\mathbf{K} \cdot \mathbf{b}}{c} - \frac{\mathbf{V}_E \cdot \mathbf{b}}{c^2} \left[1 + \frac{\hat{\mathbf{R}}_2 \cdot \mathbf{v}_2}{c} - \frac{(\mathbf{V}_E + 2\mathbf{v}_2) \cdot \mathbf{K}}{2c} \right] + \Delta T_{g,21} \right\}}{\left[\left(1 + \frac{\hat{\mathbf{R}}_2 \cdot \mathbf{v}_2}{c} \right) (1 + H) \right]}, \end{aligned} \quad (20)$$

The coordinate time \tilde{T}_0 , when the signal departed from the radio source, needs to be obtained by solving the light-time equation

$$\tilde{T}_0 = \tilde{T}_1 - \frac{\left| \tilde{\mathbf{X}}_0(\tilde{T}_0) - \tilde{\mathbf{X}}_E(\tilde{T}_1) - \mathbf{R}_{iE}(\tilde{T}_1) \right|}{c} - \Delta T_{g,01}, \quad (16)$$

where $\Delta T_{g,01}$ is the gravitational effect on the ray path from radio source S to observation station 1. It is given by (Hellings 1986; Moyer 2000, e.g.)

$$\Delta T_{g,01} = 2 \sum_J \frac{GM_J}{c^2} \ln \frac{R_{1J} + R_{0J} + R_{01}}{R_{1J} + R_{0J} - R_{01}}, \quad (17)$$

where the position of gravitating body J must be evaluated at the epoch of closest approach of the photon to the gravitating body. Higher order terms are not necessary for this purpose, because its error in the light-time solution δT only affects the VLBI delay in the order of $(V_0/c)(B/R)\delta T$, where V_0 is the coordinate velocity of the radio source. The light-time equation (Eq. 16) may be solved by numerical iteration, such as the Newton–Raphson method, and the solution converges very rapidly.

The argument of position vector in Eqs. (76) to (17) are given in TDB, however, the most usually accessible time system is UTC. UTC has the same rate with TAI, but differs by integer seconds of offset (leap seconds). Observed data at a ground station is usually time-tagged by UTC; thus we need covert time tag from UTC to TDB to get \tilde{T}_1 and \tilde{T}_0 . TAI is an atomic time-scale derived by the Bureau International des Poids et Mesures (BIPM), and it is regarded as realization of time scale of TT. Leap seconds are introduced by the IERS to keep difference between UTC and UT1 within 0.9 s in absolute value. Then TT is computed from UTC by

$$\text{TT} = (\text{TT} - \text{TAI}) + (\text{TAI} - \text{UTC}) + \text{UTC}, \quad (18)$$

where $(\text{TT} - \text{TAI})$ is 32.184 for historical reasons. $(\text{TAI} - \text{UTC})$ was 32 s in 2005 and is 33 s from 0h UTC on 1 January 2006.

Barycentric dynamical time can be computed by using time ephemeris $\Delta T_{\oplus}(T_{\text{eph}})$ (Irwin and Fukushima 1999) as

$$\text{TDB} = \text{TT} + \Delta T_{\oplus}(\text{TT}) - \Delta T_{\oplus}(\text{TT}_0) + \frac{\mathbf{V}_E \cdot \xi_1}{c^2}, \quad (19)$$

where TT_0 corresponds to 0h UT on 1 January 1977. ξ_1 is a geocentric vector to station 1 in the TT-frame. Strictly speaking, the argument of ΔT_{\oplus} is not TT, but T_{eph} . Although TDB-TT is less than 2 ms, then using TT instead of T_{eph} for the argument of ΔT_{\oplus} causes negligible error (Irwin and Fukushima 1999). Using the above procedure, the signal emission time \tilde{T}_0 and pseudo-source vector \mathbf{K} are obtained.

By using pseudo-source vector \mathbf{K} of Eq. (76) and baseline vector \mathbf{b} in the TT-frame, the VLBI delay for a radio source at finite distance is expressed in TT $(\tau_2 - \tau_1)$ as

with

$$\hat{\mathbf{R}}_2 = \frac{\mathbf{R}_2}{R_2}, R_2 = |\mathbf{R}_2|, \mathbf{V}_i = \frac{d\tilde{\mathbf{X}}_i}{d\tilde{T}}, \mathbf{v}_2 = \frac{d\mathbf{x}_2}{dt}, \quad (21)$$

where \mathbf{V}_i is coordinate velocity of object i ($= 1, 2, E$) in the TDB-frame. \mathbf{v}_2 is coordinate velocity of station 2 in GCRS. H is a correction term of the second-order of $V_2(\tilde{T}_2 - \tilde{T}_1)/c$, which represents the effect of variation of baseline vector due to the difference of arrival time. H is derived (Appendix Section) by applying Halley's method (Danby 1988, p. 151) as

$$H = \left| \frac{\mathbf{v}_2}{c} \times \hat{\mathbf{R}}_2 \right|^2 \frac{\mathbf{K} \cdot \mathbf{b}}{2R_2}. \quad (22)$$

See Appendix Section for detailed derivation of Eq. (20). $\Delta T_{g,21}$ is term of gravitational effect, and it is discussed by Klioner (1991) in detail. The gravitational effect is composed of several terms: post-Newtonian ΔT_{pN} , effect in the field of moving body ΔT_M , influence of quadruple field ΔT_Q , rotation of the bodies ΔT_R , and the post-post-Newtonian effects ΔT_{ppN} .

$$\Delta T_{g,21} = \Delta T_{pN} + \Delta T_M + \Delta T_R + \Delta T_Q + \Delta T_{ppN}. \quad (23)$$

The post-Newtonian term (ΔT_{pN}) is the most significant and it must be included at least for the Sun, Moon, and major planets (Jupiter, Saturn, Venus, Mars, and the Earth). This term is given by Eq. (43). According to Klioner (1991), the post-post-Newtonian term (ΔT_{ppN}) of the Sun becomes a few hundreds of ps in the case of grazing ray and several ps even when the source direction is 1° away from the Sun. The term ΔT_Q reaches a few tens of ps when the ray passes through the rim of Jupiter or Saturn. The term ΔT_M of Jupiter and ΔT_R of the Sun reaches 0.5 ps when ray passes the rim of those gravitating bodies. Refer to Brumberg (1987) and Klioner (1991) for the formula of each gravitational effects.

The main contribution of the wave-front curvature is concentrated in the expression of pseudo-source vector \mathbf{K} of Eq. (76) (Fukushima 1994). The effect of epoch shift due to atmospheric delay is included in the consensus model (McCarthy and Petit 2003, Eq. (11) at p. 113). We think that it must be included, but this effect is not described in this paper because it is common for any VLBI delay model.

3 Comparisons

3.1 Analytical comparison

In this section, our VLBI delay model is compared with other VLBI models. VLBI delay models for finite distance radio sources have been proposed by several authors (Fukushima 1994; Sovers et al. 1998; Klioner 1991; Moyer 2000).

Moyer's (2000) model is a direct way to compute the numerical difference of time of flight of a photon for two legs from a radio source to two observers. This model is used for the navigation of planetary probes by JPL/NASA, and it has enough precision for radio sources in the Solar System. However, it may not be practical when applied to galactic radio sources, such as pulsar and maser sources in our galaxy. Because most of the two ray paths from a radio source to observers are common in the galactic case, then a large number of digits in the numerical solution of the light-time equation will be lost when taking the difference.

Fukushima (1994) gives Lunar VLBI delay models based on BCRS, although his model is also represented by numerical iteration. Sovers et al. (1998) also presented a VLBI delay model for finite-distance radio sources for the MODEST VLBI analysis package developed by JPL. Unfortunately, they did not clearly define the reference system that the model is based on. Since their model is also described by iterative procedure, we will not make comparison here.

Klioner (1991) shows detailed consideration of VLBI delay models for several cases of radio sources at infinite and finite distances in the framework of general relativity. He discussed a VLBI delay model based on the barycentric reference system (Brumberg 1987; Kopeikin 1988). The time-scale of his reference system is TDB, thus we suppose it correspond to TDB-frame in this paper. As his model is presented in analytical form, we make analytical comparison with this model in the next section. In addition, to demonstrate the magnitude of the effect of curved wave-front, we make comparison with the consensus model as an example of a VLBI delay model for infinite distance.

3.1.1 Finite-VLBI model by Klioner (1991)

The VLBI delay model for interplanetary spacecraft derived by Klioner (1991) is expressed with our notation as follows: (A factor c^{-1} was missing from the last term of Eq. (5.1) in his paper, so it is corrected here.)

$$\begin{aligned} (\tilde{T}_2 - \tilde{T}_1)_{\text{Klioner}} = & \frac{\mathbf{K} \cdot \mathbf{B}}{c} \left[1 - \frac{\widehat{\mathbf{R}}_2 \cdot \mathbf{V}_2(\tilde{T}_1)}{c} + \frac{(\widehat{\mathbf{R}}_2 \cdot \mathbf{V}_2(\tilde{T}_1))^2}{c^2} \right] \\ & + \Delta T_{g,12} \left(1 - \frac{\widehat{\mathbf{R}}_2 \cdot \mathbf{V}_2(t_1)}{c} \right) + \frac{(\mathbf{K} \cdot \mathbf{B})}{c} H, \end{aligned} \quad (24)$$

where $\mathbf{B} = \tilde{\mathbf{X}}_2(\tilde{T}_1) - \tilde{\mathbf{X}}_1(\tilde{T}_1)$ is baseline vector in the TDB-frame. H is Halley's correction term of Eq. (22).

Klioner's delay model is given in the TDB time-scale, and conversion to the TT-scale may be provided by numerical substitution. Hence analytical comparison with our model was made in the TDB-frame. Our VLBI delay expressed in TDB is presented by Eq. (80). Infinite series expansion of this equation in terms of $\widehat{\mathbf{R}}_2 \cdot \mathbf{V}_2/c$ and H is represented as

$$\begin{aligned} (\tilde{T}_2 - \tilde{T}_1)_{\text{our}} = & \left(\Delta T_{g,12} - \frac{\mathbf{K} \cdot \mathbf{B}}{c} \right) \\ & \times \left[1 + \sum_{n=1}^{\infty} \left(-\frac{\widehat{\mathbf{R}}_2 \cdot \mathbf{V}_2}{c} \right)^n \right] \\ & \times \left[1 + \sum_{n=1}^{\infty} (-H)^n \right], \end{aligned} \quad (25)$$

where we use the same gravitational delay model as Klioner for $\Delta T_{g,12}$.

Taking into account that $H = O[(V/c)^2]$, the difference between the two models becomes

$$(\tilde{T}_2 - \tilde{T}_1)_{\text{Klioner}} - (\tilde{T}_2 - \tilde{T}_1)_{\text{our}} = \frac{\mathbf{K} \cdot \mathbf{B}}{c} \times O[(V/c)^3] \quad (26)$$

Therefore, Klioner's model is equivalent with ours to the order of $(V_E/c)^2$ in TDB. The difference is that our model gives the VLBI delay expression in the TT-scale with fully analytical formula, whereas that of Klioner gives it in TDB.

3.1.2 Consensus model (IERS conventions 2003)

The consensus model of the 2003 IERS conventions (McCarthy and Petit 2003) is widely used in the world VLBI community as the standard model. It provides the difference of arrival times between two stations in an analytical form. It is expressed with our notation as

$$(\tau_2 - \tau_1)_{\text{IERS}} = \frac{\left\{ - \left[1 - 2 \frac{W_E}{c^2} - \frac{|\mathbf{V}_E|^2 + 2\mathbf{V}_E \cdot \mathbf{v}_2}{2c^2} \right] \frac{\mathbf{k} \cdot \mathbf{b}}{c} - \frac{(\mathbf{V}_E \cdot \mathbf{b})}{c^2} \left(1 + \frac{\mathbf{k} \cdot \mathbf{V}_E}{2c} \right) + \Delta t_g \right\}}{\left[1 + \mathbf{k} \cdot \frac{\mathbf{V}_E + \mathbf{v}_2}{c} \right]}, \quad (27)$$

where \mathbf{k} is the unit vector from the Solar System barycenter (SSB) to the radio source in the TDB-frame, and Δt_g is the gravitational delay.

The IERS consensus model is originally expressed in the time-scale of TCG with baseline vectors in GCRS. However, the same formula is valid in the TT-frame for the relation between delay and baseline vector, because it is just a scale conversion (Eq. 63). Thus, here we use the consensus model in TT-scale version for comparison with our model. The effect of epoch shift due to atmospheric delay is skipped in this comparison, since that effect is common for both models. We note that the difference between \mathbf{k} and the pseudo-direction vector \mathbf{K} of Eq. (76) is the main part of the difference in the delay expression.

Now \mathbf{R}_1 is expressed with \mathbf{k} (see Fig. 2) as

$$\mathbf{R}_1 = R\mathbf{k} - \tilde{\mathbf{X}}_1 = R(\mathbf{k} - \boldsymbol{\varepsilon}_1), \quad (28)$$

where R is the distance from the SSB to the radio source and $\boldsymbol{\varepsilon}_1 \stackrel{\text{def}}{=} \tilde{\mathbf{X}}_1/R$. Then the magnitude of \mathbf{R}_1 is expanded around R as

$$R_1 = R\sqrt{1 + \boldsymbol{\varepsilon}_1^2 - 2\mathbf{k} \cdot \boldsymbol{\varepsilon}_1} = R\sqrt{1 + \boldsymbol{\varepsilon}_1^2 - 2\varepsilon_1 x_1}$$

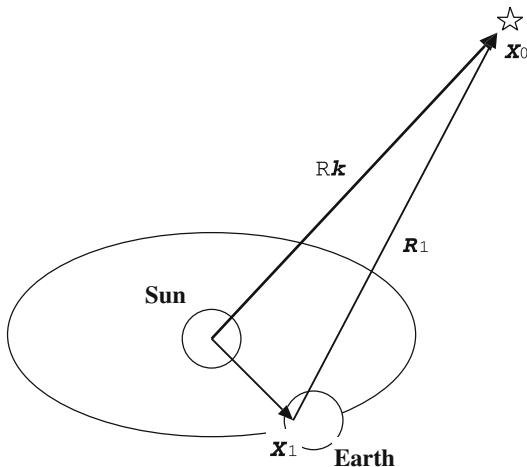


Fig. 2 Representation of the position of a radio source with the distance R and the unit vector \mathbf{k} , directed from the Solar System barycenter to the radio source

$$\begin{aligned} &= R \left\{ 1 - \varepsilon x_1 + \sum_{n=2}^{\infty} [-x_1 P_{n-1}(x_1) + P_{n-2}(x_1)] \frac{\varepsilon_1^n}{n} \right\} \\ &= R \left[1 + \frac{\varepsilon_1^2}{2} - \mathbf{k} \cdot \boldsymbol{\varepsilon}_1 - \frac{1}{2} \sum_{n=1}^{\infty} \frac{P_{2n}(0)}{n+1} (\varepsilon_1^2 - 2\mathbf{k} \cdot \boldsymbol{\varepsilon}_1)^{n+1} \right], \end{aligned} \quad (29)$$

where $x_1 = \cos \varphi_1$ and φ_1 is an angle between \mathbf{k} and vector $\boldsymbol{\varepsilon}_1$. $P_n(x)$ are Legendre polynomials, and $P_{2n}(0)$ is given by

$$P_{2n}(0) = (-1)^n \frac{(2n-1)!!}{(2n)!!}, \quad (30)$$

where $(2n)!! = 2 \cdot 4 \cdot \dots \cdot (2n-2)(2n) = n!2^n$ and $(2n-1)!! = 1 \cdot 3 \cdot 5 \cdot \dots \cdot (2n-3)(2n-1) = (2n)!/(2n)!!$.

It is seen from the second line of Eq. (29) that this infinite series converges when $\varepsilon_1 < 1$ i.e. $R > 1$ AU (astronomical unit). In the same way, R_2 can be expressed with an infinite series expansion. Then, the difference of them becomes

$$\begin{aligned} R_2(\tilde{T}_1) - R_1(\tilde{T}_1) &= -\mathbf{B} \cdot (\mathbf{k} - \boldsymbol{\varepsilon}_M) \\ &\quad \times \left[1 + \sum_{n=1}^{\infty} \frac{P_{2n}(0)}{n+1} \sum_{j=0}^n \alpha_2^j \alpha_1^{n-j} \right] \\ &\stackrel{\text{def}}{=} -\mathbf{B} \cdot (\mathbf{k} + \delta\mathbf{K}), \end{aligned} \quad (31)$$

where

$$\boldsymbol{\varepsilon}_M = \frac{(\boldsymbol{\varepsilon}_2 + \boldsymbol{\varepsilon}_1)}{2}, \quad (32)$$

$$\alpha_i = 2\mathbf{k} \cdot \boldsymbol{\varepsilon}_i - \boldsymbol{\varepsilon}_i^2, \quad (33)$$

$$\boldsymbol{\varepsilon}_i = \frac{\tilde{\mathbf{X}}_i}{R}, \quad (i = 1, 2) \quad (34)$$

and

$$\delta\mathbf{K} = -\boldsymbol{\varepsilon}_M + (\mathbf{k} - \boldsymbol{\varepsilon}_M) \sum_{n=1}^{\infty} \frac{P_{2n}(0)}{n+1} \sum_{j=0}^n \alpha_2^j \alpha_1^{n-j}. \quad (35)$$

Another expression of Eq. (31) is given with Eqs. (12) and (76) as

$$R_2(\tilde{T}_1) - R_1(\tilde{T}_1) = -\mathbf{B} \cdot \mathbf{K}. \quad (36)$$

Therefore, \mathbf{K} is expressed with \mathbf{k} and $\delta\mathbf{K}$ of Eq. (35) as

$$\mathbf{K} = \mathbf{k} + \delta\mathbf{K}. \quad (37)$$

Also, $\hat{\mathbf{R}}_2$ is expressed with \mathbf{k} and its residual as

$$\hat{\mathbf{R}}_2 = \mathbf{k} + \delta\hat{\mathbf{R}}_2, \quad (38)$$

where $\delta\hat{\mathbf{R}}_2$ is expressed with infinite series expansion in terms of α_2 or ε_2 as:

$$\begin{aligned} \delta\hat{\mathbf{R}}_2 &= -\boldsymbol{\varepsilon}_2 + (\mathbf{k} - \boldsymbol{\varepsilon}_2) \sum_{n=1}^{\infty} P_{2n}(0) \alpha_2^n \\ &= -\boldsymbol{\varepsilon}_2 + (\mathbf{k} - \boldsymbol{\varepsilon}_2) \sum_{n=1}^{\infty} P_n(x_2) \varepsilon_2^n, \end{aligned} \quad (39)$$

where $x_2 = \cos \varphi_2$ and φ_2 is an angle between \mathbf{k} and vector ε_2 . The second line of Eq. (39) shows the convergence radius of this infinite series is $\varepsilon_2 < 1$ i.e. $R > 1$ AU.

Corresponding to Eq. (80), the VLBI delay in TDB for the consensus model is given by

$$(\tilde{T}_2 - \tilde{T}_1)_{\text{IERS}} = \frac{\Delta t_g - (\mathbf{k} \cdot \mathbf{B})/c}{[1 + \mathbf{k} \cdot (\mathbf{V}_E + \mathbf{v}_2)/c]}. \quad (40)$$

Then, the time difference in TDB-scale between two models is given by using Eqs. (35), (37)–(39) and by retaining terms of order of $(V_E/c)^2$:

$$\begin{aligned} \Delta \tilde{T}_{\text{finite}} - \Delta \tilde{T}_{\text{IERS}} &= (\Delta T_{g,12} - \Delta t_g) - \frac{\delta \mathbf{K} \cdot \mathbf{B}/c}{1 + \mathbf{k} \cdot \mathbf{V}_2/c} \\ &+ \frac{\mathbf{K} \cdot \mathbf{B}}{c} \left(\frac{\delta \hat{\mathbf{R}}_2 \cdot \mathbf{V}_2}{c} + H \right) \left[1 - \frac{(\mathbf{k} + \hat{\mathbf{R}}_2) \cdot \mathbf{V}_2}{c} \right]. \end{aligned} \quad (41)$$

This is the difference of delay in TDB between our model and the consensus model. The first term is difference of gravitational delay. The gravitational term used in the consensus model has the form

$$\Delta t_g = 2 \sum_J \frac{GM_J}{c^3} \ln \frac{|\mathbf{R}_{1J}| + \mathbf{k} \cdot \mathbf{R}_{1J}}{|\mathbf{R}_{2J}| + \mathbf{k} \cdot \mathbf{R}_{2J}}. \quad (42)$$

This is approximated at the limit that the distance to the radio source is infinitely large. In the case that the radio source is at a finite distance, the same effect is computed by

$$\begin{aligned} \Delta T_{\text{pN}} &= 2 \sum_J \frac{GM_J}{c^3} \ln \left(\frac{R_{2J} + R_{0J} + R_{20}}{R_{2J} + R_{0J} - R_{20}} \right. \\ &\quad \left. \times \frac{R_{1J} + R_{0J} - R_{10}}{R_{1J} + R_{0J} + R_{10}} \right), \end{aligned} \quad (43)$$

Where positions of gravitating body J in both Eqs. (42) and (43) must be evaluated at the epoch of closest approach of the photon to the gravitating body. The difference between Δt_g and ΔT_{pN} reaches the order of nano-seconds when the ray path is close to the gravitating body (Klioner 1991). The second term of Eq. (41) contains the effect of the difference of direction vector and curvature of wave-front. The third term is the effect of variation of baseline vector due to the difference of arrival time.

When R is greater than 10 pc, then $\varepsilon_M, \varepsilon_2 \leq 5 \times 10^{-7}$. In this case, the contributions of the second and higher order terms of ε_M can be eliminated since they are less than 0.1 ps. We may then approximate $\delta \mathbf{K}$ and $\delta \hat{\mathbf{R}}_2$ simply as

$$\delta \mathbf{K} = -\mathbf{p}_M + O(\varepsilon_M^2), \quad (44)$$

$$\delta \hat{\mathbf{R}}_2 = -\mathbf{p}_2 + O(\varepsilon_2^2), \quad (45)$$

where

$$\mathbf{p}_M = \varepsilon_M - (\varepsilon_M \cdot \mathbf{k})\mathbf{k}, \quad (46)$$

$$\mathbf{p}_2 = \varepsilon_2 - (\varepsilon_2 \cdot \mathbf{k})\mathbf{k}. \quad (47)$$

We call \mathbf{p}_M the *parallax vector* for the midpoint of the baseline. It is the projection of ε_M on the plane perpendicular to \mathbf{k} (see Fig. 3).

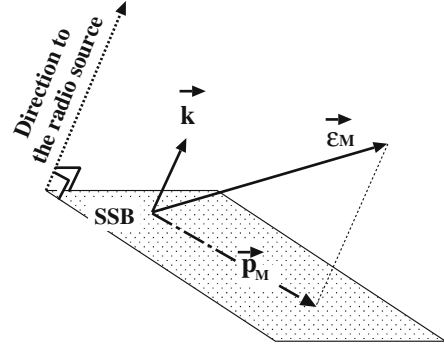


Fig. 3 Schematic view of the parallax vector, $\mathbf{p}_M \stackrel{\text{def}}{=} \varepsilon_M - (\mathbf{k} \cdot \varepsilon_M)\mathbf{k}$, where $\varepsilon_M \stackrel{\text{def}}{=} \mathbf{X}_M/R$ and R is the distance to the radio source from the Solar System barycenter(SSB)

Substituting Eqs. (44) and (45) into Eq. (41), we approximate our model in terms of parallax vectors. The delay difference of the two models in TT-scale is given by substituting Eq. (41) into Eq. (65). Eliminating higher orders than $(V_E/c)^2$, the delay difference becomes

$$\begin{aligned} \Delta \tau_{\text{finite}} - \Delta \tau_{\text{IERS}} &= (\Delta T_{g,12} - \Delta t_g) + \frac{\mathbf{b} \cdot \mathbf{p}_M}{c} \\ &\times \left(1 - \mathbf{k} \cdot \frac{\mathbf{V}_2}{c} \right) - \left(\mathbf{p}_2 \cdot \frac{\mathbf{V}_2}{c} - H \right) \frac{\mathbf{k} \cdot \mathbf{b}}{c} + O(b\varepsilon^2). \end{aligned} \quad (48)$$

The second term corresponds to the annual parallax caused by the shift of the apparent source direction. The third term comes from the variation of the baseline vector due to the difference in arrival time.

Reversing the viewpoint, Eq. (48) gives the correction terms to the consensus model when the radio sources are farther than 10 pc. The correction with these terms is enough to adapt the consensus model to observation of finite-distance radio sources with precision of 1 ps.

The annual parallax of stars has been traditionally estimated by mapping the measured celestial coordinates (α, δ) of the source at different epochs on the celestial sphere. Still the same procedure is deployed in the analysis of modern and accurate radio observation such as VLBI (e.g. Brisken et al. 2002; Chatterjee et al. 2005). We emphasize that these techniques can directly measure the parallax through model-fitting by means of Eq. (48) applied to the whole set of VLBI delay data over multiple sessions at different seasons. The partial derivative of the delay $\Delta \tau \equiv \tau_2 - \tau_1$ with respect to a parameter $p \stackrel{\text{def}}{=} a_0/R$ is explicitly given as

$$\frac{\partial \Delta \tau}{\partial p} = (\mathbf{u}_M \cdot \mathbf{b}) \left(1 - \mathbf{k} \cdot \frac{\mathbf{V}_2}{c} \right) - \left(\frac{\mathbf{u}_2 \cdot \mathbf{V}_2}{c} - \frac{\partial H}{\partial p} \right) \frac{\mathbf{k} \cdot \mathbf{b}}{c}, \quad (49)$$

where a_0 is major axis of the Earth's orbit around the Sun.

$$\mathbf{u}_i = \frac{\mathbf{X}_i}{a_0} - \left(\frac{\mathbf{X}_i \cdot \mathbf{k}}{a_0} \right) \mathbf{k}, \quad (i = 1, 2) \quad (50)$$

$$\mathbf{u}_M = \frac{\mathbf{u}_1 + \mathbf{u}_2}{2}. \quad (51)$$

The vector \mathbf{u}_l , ($l = 1, 2, M$) is projection of \mathbf{X}_l/a_0 to a plane perpendicular to the vector \mathbf{k} . $\partial H/\partial p$ is smaller than the other term by factor of V_E/c , thus it may be neglected. The partial derivative of Eq. (49) will be useful to estimate parameter $p = a_0/R$ with the weighted least-square method from delay data set.

3.2 Numerical comparison with consensus model

In this section, the difference between our model and the IERS consensus model is evaluated numerically in some practical cases. Figure 4 shows the maximum difference for a relatively long baseline, Kashima–Algonquin (9,000 km).

In the case of α Cen. ($R = 1.3$ pc), which is known as the nearest star system to Earth, the maximum difference amounts to some 100 ns. This effect will be also detectable for radio sources in our galaxy such as pulsars. A good example is the millisecond pulsar PSR1937+21 ($R \sim 3.6$ kpc), the use of which has been discussed for the purpose of the reference frame tie between the ICRF and dynamical reference frames (Bartel et al. 1996; Chatterjee and Codes 2000; Petit 1994). In that case, the delay difference between our model and the consensus model, $\tau_{\text{finite}} - \tau_{\text{IERS}}$, is illustrated in Fig. 5 for the Kashima–Algonquin baseline. The difference consists of oscillations with the amplitude about 40 ps at maximum. These are caused by the two components in Eq. (48), \mathbf{p}_M and \mathbf{p}_2 . From another point of view, this shows that the distance to the pulsar may be directly estimated by analyzing the delays with the new model.

Let us move next to a closer case. The consensus model is designed for observation of extra-galactic radio sources, and cannot be used for radio sources in the Solar System, as stated in the 2003 IERS Conventions (McCarthy and Petit 2003, p. 109). If we use the direction vector of a radio source starting from the SSB in the consensus model, the difference is so large that it is obviously nonsense to use the consensus model for object in the Solar System.

However, if geocentric direction vector to a radio source is used instead of unit vector from SSB, the error becomes smaller. Actually this approach was taken by Sovers et al. (1998) to make VLBI delay model for finite-distance radio source. To demonstrate the effect of curved wave-front in this case, here we rename this geocentric direction vector as \mathbf{k} and substitute it to the consensus model. The difference of two models is depicted for Venus in the period of 2005–2007 in Fig. 6. The main term of the difference is the so-called *horizontal parallax*.

4 Conclusion

A delay model for Earth-based VLBI observation of finite-distance radio sources has been developed. VLBI delay in TT is expressed by fully analytical formula. The curvature of the wave-front of the radio signal was taken into account by using pseudo-source vector \mathbf{K} . The effect on variation of baseline

vector due to the difference of arrival time was approximated with Halley's method (Appendix section). The model has precision better than 1 ps for any radio source above the altitude of 100 km from the ground in ground-based VLBI observations. Since Earth satellites are recommended to be analyzed in the GCRS (McCarthy and Petit 2003, Sect. 10.2), our model may not be used for Earth satellites. However our model might be useful in VLBI observation of Earth swing-by of interplanetary spacecraft.

This new delay model was derived with intention for practical use in VLBI analysis software to analyze observed VLBI data of spacecraft. For that reason, coordinates of spacecraft and planets are supposed to be given in TDB-frame (e.g. JPL ephemerides). We have tried to include all of the equations and relations necessary for coding a computer program, except for the terms of gravitational delay in Eq. (23). ΔT_{pN} is given in Eq. (43), although other terms have to be taken from the original literature. They may be taken into account for VLBI observations of a spacecraft that is landing or orbiting a planet.

When the distance to the radio source is larger than 10 pc, the difference between our model and consensus model is expressed by a few terms. Therefore, the consensus model can be adapted for VLBI observation of finite-distance radio sources by using these correction terms. This is a significant advantage for implementing the delay model for finite-distance radio source into current VLBI analysis software, such as CALC/SOLVE or OCCAM. The analytical expressions of the parallax effects may enable modeling and direct estimate of the parallax from global analysis of VLBI data sets.

Numerical comparison between our model and the consensus model indicated that the difference is significant for the radio sources in our galaxy (< 20 kpc). The effect of the curved wave-front was demonstrated for PSR1937+21 and Venus with Kashima–Algonquin baseline as example.

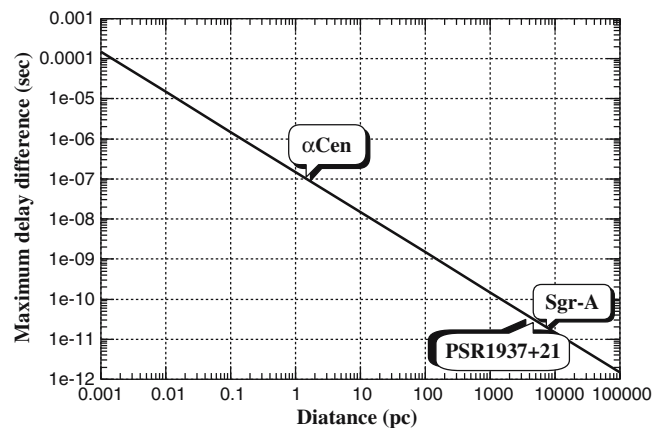


Fig. 4 Maximum difference of $\tau_{\text{finite}} - \tau_{\text{IERS}}$ plotted as a function of distance for the Kashima–Algonquin baseline (9,000 km) as an example. This plot was made for configuration on a virtual source in the direction of the north pole ($\delta = 90^\circ$). We confirmed that there was no significant dependence on the declination

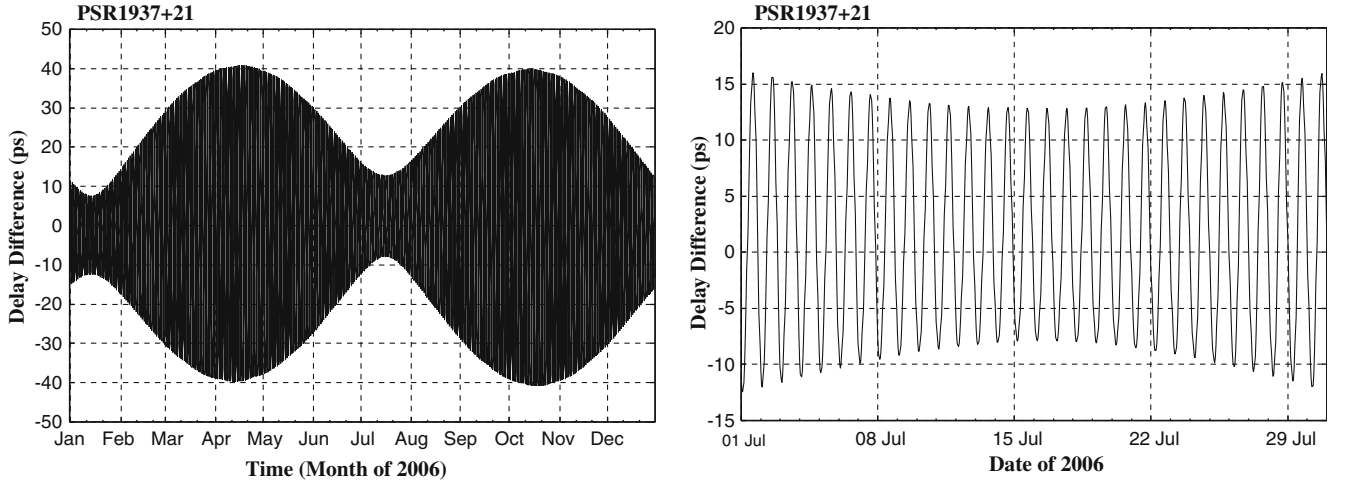


Fig. 5 Difference in the delay time between the finite-VLBI model and the consensus model, evaluated for PSR1937+21 ($\alpha = 19^{\text{h}}39^{\text{m}}38^{\text{s}}.56$, $\delta = +21^{\circ}34'59''14$, $d = 3.6$ kpc) for the Kashima–Algonquin baseline as a function of epoch in 2005 (*left panel*). The data in July is magnified in the *right panel* to more clearly show its daily variation

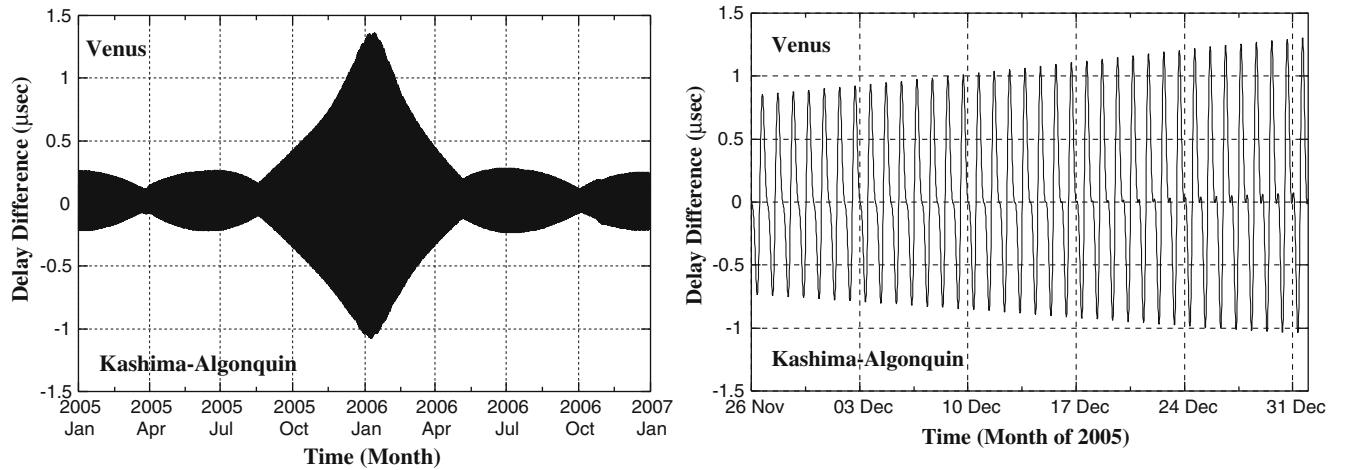


Fig. 6 The effects of the curved wave-front for Venus with the Kashima–Algonquin baseline in 2005 (*left panel*). The geocentric vector to Venus is substituted instead of barycentric vector \mathbf{k} in the consensus model, and the delay difference from our finite-distance VLBI model is plotted. A magnified plot for the period of December 2005 is in the *right panel*

A Appendix: Derivation of delay model for finite-distance radio source

A.1 Reference system and coordinate transformation

The Barycentric Celestial Reference System (BCRS) and Geocentric Celestial Reference System (GCRS) are recommended in the 2003 IERS Conventions (McCarthy and Petit 2003) as fundamental reference system in framework of general relativity. The time-coordinate of BCRS and GCRS are named, respectively, Barycentric Coordinate Time (TCB) and Geocentric Coordinate Time (TCG). Metric tensors of each of these reference systems are given by Eqs. (1) and (3), where we denote space-time coordinates of BCRS by (T, \mathbf{X}) , and that of GCRS by (t, \mathbf{x}) .

In this section, we derive VLBI delay model for radio source at finite distance. When radio source is in the Solar System, we suppose its position is given in the BCRS. In fact, orbits of planets, asteroids and most of spacecraft in the solar system are currently described in the DE405 planetary ephemeris, which is developed by JPL/NASA and it is recommended as an IERS standard McCarthy and Petit 2003, Chapt. 3. Here we call this reference system as TDB-frame, since space-time coordinate of JPL ephemeris is consistent with TDB (see Sect. 2.1). TDB-frame is a system differing from BCRS by a constant factor L_B . The metric of TDB-frame is given by Eq. (11), where space-time coordinates of TDB-frame is denoted by $(\tilde{T}, \tilde{\mathbf{X}})$. We assume radio sources outside the Solar System may also be given in the TDB-frame.

The time interval observed at ground station is measured by local clock running as proper time at that point. That time scale is usually different from terrestrial time (TT), since local gravitational potential at the observatory usually differs from that of geoid. Although the difference of time scale (clock rate) caused by difference of gravitational potential is absorbed in the process used to keep the local clock synchronized with UTC. Therefore, hereafter time scale of observed delay at observatory is regarded as that of TT.

For practical use, we define TT-frame, which is a geocentric reference system differing from GCRS by a factor of L_G From Eq. (5). The metric of TT-frame is given by Eq. (6), where space-time coordinates of TT-frame are denoted by (τ, ξ) . Geocentric station coordinates are converted from International Terrestrial Reference Frame (ITRF), which is a reference frame co-rotating with the Earth, to the TT-frame by coordinate transformation due to diurnal motion, polar motion, nutation, and precession (Chapt. 5 of McCarthy and Petit 2003). Note that the concept of ITRS is defined in scale of GCRS; however products of ITRF is expressed in TT-scale rather than TCG-scale, except for ITRF94, ITRF96, and ITRF97. Then the scales of reference frames differ by factor of L_G depending on the version of ITRF. The scale conversion from TT-scale to TCG-scale is explicitly given in Eq. (14) of (McCarthy and Petit 2003, p. 30). Hereafter we assume that station coordinates are expressed in TT-scale (e.g. ITRF2000) and station coordinates are transformed to celestial reference frame (TT-frame) without scale change.

The coordinate transformation from BCRS (T, \mathbf{X}) to the GCRS (t, \mathbf{x}) is recommended by Resolution B1.3 adopted at the XXIV IAU General Assembly (Soffel et al. 2003). This is expressed with our notation as

$$\begin{aligned} t(T, \mathbf{X}) = & T - \frac{1}{c^2} \left[A(T) + V_E^i(T) R_E^i(T, \mathbf{X}) \right] \\ & + \frac{1}{c^4} \left[B(T) + B^i(T) R_E^i(T, \mathbf{X}) \right. \\ & \left. + B^{ij}(T) R_E^i(T, \mathbf{X}) R_E^j(T, \mathbf{X}) + C(T, \mathbf{X}) \right] + O(c^{-5}), \end{aligned} \quad (52)$$

$$\begin{aligned} x^i(T, \mathbf{X}) = & R_E^i(T, \mathbf{X}) \\ & + \frac{1}{c^2} \left[\frac{1}{2} V_E^i(T) V_E^j(T) R_E^j(T, \mathbf{X}) + W_E(\mathbf{X}_E(T)) R_E^i(T, \mathbf{X}) \right. \\ & \left. + R_E^i(T, \mathbf{X}) A_E^j(T) R_E^j(T, \mathbf{X}) - \frac{1}{2} A_E^i(T) R_E^2(T, \mathbf{X}) \right] \\ & + O(c^{-4}), \end{aligned} \quad (53)$$

where $R_E^i(T, \mathbf{X}) = X^i - X_E^i(T)$ and

$$A(T) = \int_{T_0}^T \left[\frac{1}{2} V_E^2(T') + W_E(\mathbf{X}_E(T')) \right] dT', \quad (54)$$

$$\begin{aligned} B(T) = & \int_{T_0}^T \left[-\frac{1}{8} V_E^4(T') - \frac{3}{2} V_E^2(T') W_E(\mathbf{X}_E(T')) \right. \\ & \left. + 4V_E^i(T') W_E^i(\mathbf{X}_E(T')) + \frac{1}{2} W_E^2(\mathbf{X}_E(T')) \right] dT', \end{aligned} \quad (55)$$

$$B^i(T) = -\frac{1}{2} V_E^2(T) V_E^i(T) + 4W_E^i(\mathbf{X}_E) - 3V_E^i(T) W_E(\mathbf{X}_E(T)), \quad (56)$$

$$\begin{aligned} B^{ij}(T) = & -V_E^i(T) \delta_{aj} Q^a(T) + 2 \frac{\partial}{\partial X^j} U_E^i(\mathbf{X}_E(T)) \\ & - V_E^i \frac{\partial}{\partial X^j} W_E(\mathbf{X}(T)) + \frac{1}{2} \delta^{ij} \dot{W}_E(\mathbf{X}_E(T)), \end{aligned} \quad (57)$$

$$C(T, \mathbf{X}) = -\frac{1}{10} R_E^2(T, \mathbf{X}) (\dot{A}_E^i(T) R_E^i(T)), \quad (58)$$

$$Q^a = \delta_{ai} \left[\frac{\partial}{\partial X^i} W_E(\mathbf{X}_E(T)) - A_E^i(T) \right]. \quad (59)$$

Here X_E^i , V_E^i , and A_E^i are the vector components of position, coordinate velocity, and coordinate acceleration of the Earth in the BCRS, the dot over the quantities stands for the derivative with respect to coordinate time. T_0 represents the epoch of 1 January 1977, 0^h0^m0^s. The external potentials W_E and W_E^i are given by

$$\begin{aligned} W_E(T, \mathbf{X}) = & G \sum_{J \neq E} \int \frac{\sigma(T, \mathbf{X}')}{|\mathbf{X} - \mathbf{X}'|} d^3 X' \\ & + \frac{1}{2c^2} G \sum_{J \neq E} \frac{\partial^2}{\partial T^2} \int \sigma(T, \mathbf{X}') |\mathbf{X} - \mathbf{X}'| d^3 X', \end{aligned} \quad (60)$$

$$W_E^i(T, \mathbf{X}) = G \sum_{J \neq E} \int \frac{\sigma^i(T, \mathbf{X}')}{|\mathbf{X} - \mathbf{X}'|} d^3 X', \quad (61)$$

where E stands for the Earth, J runs for all gravitational bodies in the Solar System, except for the Earth. σ and σ^i are the gravitational mass and current densities, respectively.

Let us suppose a signal that departed from a radio source at (T_0, \mathbf{X}_0) arrives to observation station 1 and 2 at (T_1, \mathbf{X}_1) and (T_2, \mathbf{X}_2) in BCRS. These events correspond to space-time coordinates $(\tilde{T}_0, \tilde{\mathbf{X}}_0)$, $(\tilde{T}_1, \tilde{\mathbf{X}}_1)$, and $(\tilde{T}_2, \tilde{\mathbf{X}}_2)$ in the TDB-frame (Fig. 1). The last two events respectively correspond to (t_1, \mathbf{x}_1) and (t_2, \mathbf{x}_2) in the GCRS and to (τ_1, ξ_1) and (τ_2, ξ_2) in the TT-frame. In case of ground-based VLBI observation, the time interval of signal arrival to two observatories on the Earth is less than 43 ms. Then approximation up to the order of $(V_E/c)^2$ is enough for 1 ps accuracy.

By using Eqs. (52) and (53), temporal interval between two events (T_1, \mathbf{X}_1) and (T_2, \mathbf{X}_2) is expressed in TCG as

$$\begin{aligned} t_2 - t_1 = & (T_2 - T_1) \left[1 - \frac{1}{c^2} \left(\frac{1}{2} V_E^2 + W_E \right) \right] \\ & - \frac{V_E^i (x_2^i(t_1) - x_1^i(t_1)) + v_2^i (t_2 - t_1)}{c^2}, \end{aligned} \quad (62)$$

where coordinate velocity of the Earth (V_E^i) and external gravitational potential (W_E) is approximated as constant in the integral of Eq. (54) for the short time interval of the two events. Also, contributions from accelerations due to the Earth's spin and orbital motion were eliminated, since they are, respectively, about 3.3 cm/s² and 6 mm/s². Then $x_2^i(t_2) - x_1^i(t_1)$ is approximated as $x_2^i(t_1) - x_1^i(t_1) + v_2^i(t_2 - t_1)$.

From the definition of TT-frame, its temporal and spatial scale differs from that of GCRS by the constant factor L_G as

$$\begin{aligned} (\tau_2 - \tau_1) = & (1 - L_G)(t_2 - t_1) \\ \xi^i = & (1 - L_G)x^i. \end{aligned} \quad (63)$$

Also coordinates components of TDB-frame differ from that of BCRS by the constant factor L_B as

$$\begin{aligned} (\tilde{T}_2 - \tilde{T}_1) &= (1 - L_B)(T_2 - T_1) \\ \tilde{X}^i &= (1 - L_B)X^i. \end{aligned} \quad (64)$$

With these factors and Eq. (8), Eq. (62) is re-written as a relation between TT and TDB as follows:

$$\begin{aligned} \tau_2 - \tau_1 &= \frac{\tilde{T}_2 - \tilde{T}_1}{1 - L_C} \left[1 - \frac{1}{c^2} \left(\frac{1}{2} |\mathbf{V}_E|^2 + \mathbf{V}_E \cdot \mathbf{v}_2 + W_E \right) \right] \\ &\quad - \frac{\mathbf{V}_E \cdot \mathbf{b}}{c^2}, \end{aligned} \quad (65)$$

where

$$b^i = \xi_2^i(\tau_1) - \xi_1^i(\tau_1) \quad (66)$$

is the baseline vector in TT-frame, and \mathbf{v}_2 is coordinate velocity of station 2, and its value is identical in either of TT-frame and GCRS.

When the baseline vector in BCRS $X_2^i(T_1) - X_1^i(T_1)$ is concerned, space-time coordinates of event (T_1, \mathbf{X}_1) correspond to (t_1, \mathbf{x}_1) , although (T_1, \mathbf{X}_2) does not correspond to (t_1, \mathbf{x}_2) , but corresponds to $(t_1 + \delta t_1, \mathbf{x}_2)$, where δt_1 is difference of simultaneity between BCRS and GCRS. The difference in order of $(V_E/c)^2$ is given from Eq. (52) as

$$\delta t_1 = -\frac{V_E^i(X_2^i - X_1^i)}{c^2}. \quad (67)$$

Then a relation between baseline in BCRS $X_2^i(T_1) - X_1^i(T_1)$ and that in GCRS $x_2^i(t_1) - x_1^i(t_1)$ is derived from Eq. (53) in the order of $(V_E/c)^2$ as

$$\begin{aligned} x_2^i(t_1) - x_1^i(t_1) &= (X_2^i(T_1) - X_1^i(T_1)) \left(1 + \frac{W_E}{c^2} \right) \\ &\quad + \frac{V_E^j (X_2^j(T_1) - X_1^j(T_1))}{c^2} \left(\frac{V_E^i}{2} + v_2^i \right). \end{aligned} \quad (68)$$

Converting Eq. (68) by using relations of Eqs. (63) and (64), the baseline vector in TT-frame $\xi_2(\tau_1) - \xi_1(\tau_1)$ is expressed with that of TDB-frame $\tilde{X}_2(\tilde{T}_1) - \tilde{X}_1(\tilde{T}_1)$ as

$$b^i = \frac{B^i}{1 - L_C} \left(1 + \frac{W_E}{c^2} \right) + \frac{V_E^j B^j}{c^2} \left(\frac{V_E^i}{2} + v_2^i \right), \quad (69)$$

where

$$B^i = \tilde{X}_2^i(\tilde{T}_1) - \tilde{X}_1^i(\tilde{T}_1). \quad (70)$$

Since the difference between \mathbf{B} and \mathbf{b} is of the order of $(V_E/c)^2$, \mathbf{B} is expressed with \mathbf{b} to the order of $(V_E/c)^2$ from Eq. (69) as

$$B^i = b^i \left(1 - \frac{W_E}{c^2} - L_C \right) - \frac{V_E^j b^j}{c^2} \left(\frac{V_E^i}{2} + v_2^i \right), \quad (71)$$

where we used the same notation of coordinate velocity \mathbf{V}_E and gravitational potential W_E for BCRS and TDB-frame, since these quantities are free from scale change as far as the speed of light is constant.

A.2 Derivation of finite distance VLBI delay with Halley's method

The problem to be solved is computing the delay $\tau_2 - \tau_1$ at given epoch τ_1 under the conditions that the coordinates of the radio source and orbits of planets, including the Earth, are given as a function of time in the TDB-frame. The signal departs from a radio source at $(\tilde{T}_0, \tilde{\mathbf{X}}_0)$ arrives at observer 1 at $(\tilde{T}_1, \tilde{\mathbf{X}}_1)$. The epoch \tilde{T}_0 must be solved from light-time equation (Eq. 16) with Eq. (17).

The position vector from radio source in TDB-frame $(\tilde{T}_0, \tilde{\mathbf{X}}_0)$ to observation station 2 $(\tilde{T}_2, \tilde{\mathbf{X}}_2)$ can be approximated with coordinate velocity \mathbf{V}_2 as

$$\mathbf{R}_2(\tilde{T}_2) = \mathbf{R}_2(\tilde{T}_1) - \mathbf{V}_2(\tilde{T}_2 - \tilde{T}_1), \quad (72)$$

where \mathbf{R}_2 is defined with Eq. (13). Effects of the acceleration of station 2 are ignored, since the error due to this approximation is $30 \mu\text{m}$ at maximum.

The magnitude of $\mathbf{R}_2(\tilde{T}_2)$ is expanded around that of $\mathbf{R}_2(\tilde{T}_1)$ as

$$\begin{aligned} R_2(\tilde{T}_2) &= R_2(\tilde{T}_1) \left\{ 1 - \hat{\mathbf{R}}_2 \cdot \frac{\mathbf{V}_2(\tilde{T}_2 - \tilde{T}_1)}{R_2} \right. \\ &\quad + \frac{|\mathbf{V}_2 \times \hat{\mathbf{R}}_2|^2}{2R_2^2} (\tilde{T}_2 - \tilde{T}_1)^2 \\ &\quad \left. + \frac{|\mathbf{V}_2 \times \hat{\mathbf{R}}_2|^2}{2R_2^3} (\hat{\mathbf{R}}_2 \cdot \mathbf{V}_2) (\tilde{T}_2 - \tilde{T}_1)^3 + \dots \right\}, \end{aligned} \quad (73)$$

where $R_2 = |\mathbf{R}_2|$ and $\hat{\mathbf{R}}_2 = \mathbf{R}_2/R_2$. Time tags for these variables are omitted but it is \tilde{T}_1 such as $R_2 = R_2(\tilde{T}_1)$, $\hat{\mathbf{R}}_2 = \hat{\mathbf{R}}_2(\tilde{T}_1)$, and $\mathbf{V}_2 = \mathbf{V}_2(\tilde{T}_1)$.

The third-order term of Eq. (73) is evaluated as follows:

$$\begin{aligned} \frac{|\mathbf{V}_2 \times \hat{\mathbf{R}}_2|^2}{2R_2^3} (\hat{\mathbf{R}}_2 \cdot \mathbf{V}_2) (\tilde{T}_2 - \tilde{T}_1)^3 &\leq \frac{|\mathbf{V}_2| (\tilde{T}_2 - \tilde{T}_1)^3}{3\sqrt{3} R_2^3} \\ &= \frac{1}{3\sqrt{3}} \left(\frac{|\mathbf{V}_2|}{c} \right)^3 \left| \frac{R_2 - R_1}{R_2} \right|^3, \end{aligned} \quad (74)$$

where $\tilde{T}_2 - \tilde{T}_1 \approx (R_2 - R_1)/c$ was substituted. The truncation error by omitting the third-order term was evaluated by this inequality under the condition that mutual visibility from the Earth-based stations is kept. Figure 7 shows that the truncation error is less than 0.1 ps for any space object above the altitude of 100 km in case of the Earth-based VLBI observations.

Then the time interval $\tilde{T}_2 - \tilde{T}_1$ can be expressed with sufficient accuracy by using Eq. (73) as

$$\begin{aligned} c(\tilde{T}_2 - \tilde{T}_1) &= R_2(\tilde{T}_2) - R_1(\tilde{T}_1) + c\Delta T_g, \\ &= c\Delta T_{g,12} - \mathbf{K} \cdot \mathbf{B} - \hat{\mathbf{R}}_2 \cdot \mathbf{V}_2(\tilde{T}_2 - \tilde{T}_1) \\ &\quad + \frac{|\mathbf{V}_2 \times \hat{\mathbf{R}}_2|^2}{2R_2} (\tilde{T}_2 - \tilde{T}_1)^2, \end{aligned} \quad (75)$$

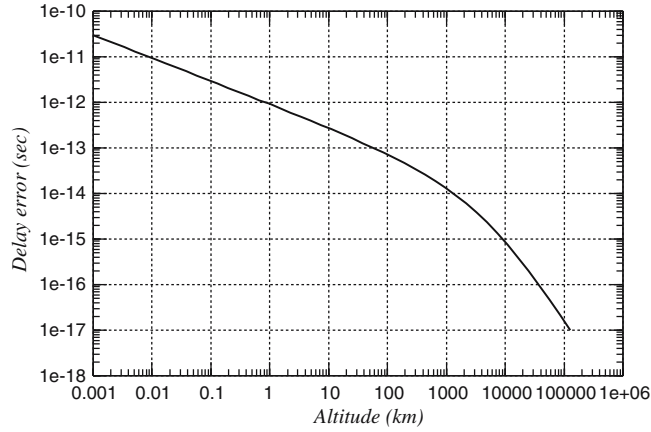


Fig. 7 Maximum of the third-order truncation error, $R_2 |V_2(R_2 - R_1)/\sqrt{3}cR_2|^3$ evaluated as a function of the altitude of the source. The evaluation took into account mutual visibility of ground-based VLBI observers

where \mathbf{K} is the pseudo-direction vector, which was introduced by Fukushima (1994), and \mathbf{B} is the baseline vector defined in the TDB-frame.

$$\mathbf{K} = \frac{\mathbf{R}_1(\tilde{T}_1) + \mathbf{R}_2(\tilde{T}_1)}{R_1(\tilde{T}_1) + R_2(\tilde{T}_1)},$$

$$\mathbf{B} = \tilde{\mathbf{X}}_2(\tilde{T}_1) - \tilde{\mathbf{X}}_1(\tilde{T}_1), \quad (76)$$

where \mathbf{R}_i ($i = 1, 2$) is computed by Eq. (13). Equation (75) is rewritten in the order of $(\tilde{T}_2 - \tilde{T}_1)$ as

$$\frac{|V_2|^2 - (\hat{\mathbf{R}}_2 \cdot V_2)^2}{2R_2} (\tilde{T}_2 - \tilde{T}_1)^2 - (c + \hat{\mathbf{R}}_2 \cdot V_2)(\tilde{T}_2 - \tilde{T}_1) + c\Delta T_{g,12} - \mathbf{K} \cdot \mathbf{B} = 0. \quad (77)$$

In general, when a quadratic equation is given as

$$\frac{1}{2}f''x^2 + f'x + f^0 = 0, \quad (78)$$

its approximation solution is obtained by

$$x = \frac{-f^0}{f' [1 - f^0 f'' / 2(f')^2]}. \quad (79)$$

This is called Halley's method (Danby 1988, p. 151). This approximation is known to give third-order convergence in iterative use to solve a quadratic equation. It is quite effective, especially when $f'' f^0 \ll (f')^2$, as is the case here.

The solution of Eq. (77) is obtained by using Halley's method as

$$\tilde{T}_2 - \tilde{T}_1 = \frac{\Delta T_{g,12} - (\mathbf{K} \cdot \mathbf{B})/c}{[1 + (\hat{\mathbf{R}}_2 \cdot V_2)/c] \left\{ 1 + \frac{\mathbf{K} \cdot \mathbf{B} [|V_2|^2 - (\hat{\mathbf{R}}_2 \cdot V_2)^2]}{2c^2 R_2 [1 + (\hat{\mathbf{R}}_2 \cdot V_2)/c]^2} \right\}}$$

$$= \frac{\Delta T_{g,12} - (\mathbf{K} \cdot \mathbf{B})/c}{(1 + \hat{\mathbf{R}}_2 \cdot V_2/c)(1 + H)}. \quad (80)$$

where H is the correction term due to Halley's method, which is expressed in the order of $(V_E/c)^2$ as

$$H \stackrel{\text{def}}{=} \frac{\mathbf{K} \cdot \mathbf{B} |V_2 \times \hat{\mathbf{R}}_2|^2}{2R_2 c^2} \approx \frac{\mathbf{K} \cdot \mathbf{b} |V_2 \times \hat{\mathbf{R}}_2|^2}{2R_2 c^2}. \quad (81)$$

The approximation error of Halley's method is evaluated by

$$\delta x \cong \frac{[(f^0)^3 f''^2]}{4f'^5} \simeq \left(\frac{B}{4c}\right) \left(\frac{B}{R_2}\right)^2 \left(\frac{V_2}{c}\right)^4. \quad (82)$$

Since the order of the error is $(V_2/c)^4$, then it is negligible.

Substituting Eq. (71) into Eq. (80) and into Eq. (65), the VLBI delay model for a radio source at finite distance is obtained in the order of $(V_E/c)^2$ as:

$$(\tau_2 - \tau_1)_{\text{Finite}} = \frac{\left\{ -\left[-2\frac{W_E}{c^2} - \frac{|V_E|^2 + 2V_E \cdot v_2}{2c^2} \right] \frac{\mathbf{K} \cdot \mathbf{b}}{c} - \frac{V_E \cdot \mathbf{b}}{c^2} \left[1 + \frac{\hat{\mathbf{R}}_2 \cdot V_2 - (V_E + 2v_2) \cdot \mathbf{K}}{2c} \right] + \Delta T_{g,21} \right\}}{\left[(1 + \frac{\hat{\mathbf{R}}_2 \cdot V_2}{c})(1 + H) \right]}.$$

Acknowledgements We thank Dr Yoshikawa of JAXA/ISAS and Kashima VLBI group of NICT for guiding us to the issue of finite VLBI observation. We also appreciate Prof W. Cannon of York University, Canada, for care of this work during author's stay in his laboratory. Finally, we appreciate S. A. Klioner, H. Schuh and referees of Journal of Geodesy for precise checks, useful comments, and constructive criticism. Owing to them, the content of this paper was greatly improved.

References

- Bartel N, Chandler JF, Ratner MI, Shapiro II, Pan R, Cappallo RJ (1996) Towards a frame-tie via millisecond pulsar VLBI. *Astron J* 112:1690–1696
- Border JS, Donovan FF, Finley SG, Hildebrand CE, Moultrie B, Skjerve LJ (1982) Determining spacecraft angular position with delta VLBI: the voyager demonstration. *AIAA/AAS Astrodynamics Conference*, 9-11 August, San Diego, CA, AIAA-82-1471
- Briskin WF, Benson JM, Goss WM, Thorsett SE (2002) Very long baseline array measurement of nine pulsar parallaxes. *Astrophys J* 571:906–917
- Brumberg VA (1987) Post-post-Newtonian propagation of light in the Schwarzschild field. *Kinematica Fizika Neb* 3(1):8–13
- Charlot P (2004) The ICRF: 2010 and beyond. In: Vandenberg NR, Baver KD, (eds) *Proceedings of International VLBI service for geodesy and astrometry 2004 general meeting*, NASA/CP-2004-212255; pp. 12–21

- Chatterjee S, Vlemmings WHT, Briskin WF, Lazio TJW, Cordes JM, Goss WM, Thorsett SE, Fomalont EB, Lyne AG, Kramer M (2005) Getting its kicks: a VLBA parallax for the hyperfast pulsar B1508+55. *Astrophys J* 630:L61–L64
- Chatterjee S, Codes JM (2000) VLBI neutron star astrometry: techniques and initial results. In: Kramer M, Wex N, Wielebinski R (eds) *IAU colloquium 177: pulsar astronomy – 2000 and beyond*, ASP conference Service, vol 202, pp 139–140
- Danby JMA (1988) *Fundamentals of celestial mechanics*, 2nd edn. Willmann-Bell, Richmond, 151pp
- Eubanks TM (1991) A Consensus model for relativistic effects in geodetic VLBI. In: *Proceedings of the USNO workshop on relativistic models for use in space geodesy*, pp. 60–82
- Fukushima T (1994) Lunar VLBI observation model. *Astron Astrophys* 291: 320-323
- Guinot B, Sidelmann PK (1988) Time scales – Their history, definition and interpretation. *Astron Astrophys* 194: 304-308
- Heki K, Matsumoto K, Floberghagen R (1999) Three-dimensional tracking of a lunar satellite with differential very-long-baseline-interferometry. *Adv Space Res* 23:1821-1824
- Hellings RW (1986) Relativistic effects in astronomical timing measurements. *Astron J* 91:650–659
- Irwin AW, Fukushima T (1999) A numerical time ephemeris of the Earth. *Astron Astrophys* 348:642–652
- Kobayashi, H, Kawaguchi N, Manabe S, Omodaka T, Kameya O, Shibata KM, Miyaji T, Honma M, Tamura Y, Hirota T, Imai H, Kuji S, Horiai K, Sakai S, Sato S, Iwadate K, Kanya Y, Jike T, Fujii T, Kasuga T (2004) VERA system. In: Bachiler R, Colomer F, Desmurs JF, de Vicente P (eds) *Proceedings of the 7th Symposium of the European VLBI network*, 12–15 October, Toledo, Spain, pp 275–278
- Kopeikin SM, (1988) Celestial coordinate reference systems in curved space-time. *Cel Mech* 44:87–115
- Klioner S (1991) General relativistic model of VLBI observables. In: Carter WE (eds) *Proceedings of AGU Chapman conference on geodetic VLBI: monitoring of global change*. NOAA Technical Report NOS 137 NGS 49, American Geophysical Union, Washington DC, pp 188–202
- Lebreton J-P, Matson DL (2002) The Huygens probe: science, payload and mission overview. *Space Sci Rev* 104:59–100
- Matsumoto K, Heki K, Rowlands DD (1999) Impact of far-side satellite tracking on gravity estimation in the SELENE project. *Adv Space Res* 23:1809–1812
- McCarthy DD, Petit G (2003) *IERS conventions*. IERS Technical Note No. 32, Paris Observatory
- Moyer TD (2000) *Formulation for observed and computed values of deep space 4 network data types for navigation*. JPL Monograph 2 (JPL Publication 00-7). This is published from JPL deep space communications and navigation series, John Wiley, Hoboken, ISBN 0-471-44535-5
- Sekido M., Ichikawa R, Osaki H, Kondo T, Koyama Y, Yoshikawa M, Ohnishi T, Cannon WH, Novikov A, Berube M (2004) Astrometry observation of spacecraft with very long baseline interferometry – a step of VLBI application for spacecraft navigation. In: Noon D (ed) *Proceedings of URSI commission-F triennium open symposium*, 1–4 June, Cairns, Australia, pp. 163-170 (<http://www.ursi-f2004.com/>)
- Petit G (1994) *Observations VLBI Des Pulsars Millisecondes Pour le Raccordement des Systèmes de Référence Célestes et la Stabilité des Échelles de Temps*, PhD thesis, Paris Observatory
- Petrov L (2005) Mark-5 VLBI analysis software Calc/Solve (<http://gemini.gsfc.nasa.gov/solve/>)
- Shahid-Saless B, Hellings RW (1991) A picosecond accuracy relativistic VLBI model via fermi normal coordinates. *Geophys Res Lett* 8:1139–1142
- Soffel MH, Muller J, Wu X, Xu C (1991) Consistent relativistic VLBI theory with picosecond accuracy. *Astron J* 101:2306–2310
- Soffel M, Klioner SA, Petit G, Wolf P, Kopeikin SM, Bretagon P, Brumberg VA, Capitaine N, Damour T, Fukushima T, Guinot B, Huang T-Y, Lindgren L, Ma C, Nordvedt K, Ries JC, Seidelmann PK, Vokrouhlicky D, Will CM, Xu C (2003) The IAU resolutions for astrometry, celestial mechanics, and meteorology in the relativistic framework: explanatory supplement. *Astron J* 126:2687–2706
- Sovers OJ, Fanselow JL, Jacobs CS (1998) Astrometry and geodesy with radio interferometry: experiments, models, results. *Rev. Mod Phys* 70(4):1393–1454
- Standish EM (1998) JPL planetary and lunar ephemerides, DE405/LE405, JPL IOM 312.F-98-048
- Standish EM (1998b) Time scale in the JPL and CfA ephemerides. *Astron Astrophys* 336:381-384
- Titov O, Tesmer V, Boehm J (2004) OCCAM 6.0 User's Guide (<http://www.ga.gov.au/geodesy/sgc/vlbi/>)
- Yamamoto T, Tsuruda K (1998) The PLANET-B mission. *Earth Planets Space* 50: 175–181
- Zhu SY, Groten E (1988) Relativistic effects in VLBI time delay measurement. *Manuscripta Geodetica* 13:33–39